AGU PUBLICATIONS

Geophysical Research Letters

RESEARCH LETTER
10.1002/2017GL073038

Key Points:
- A few periodicities (~30 and 60 min) in IMF B_z predominantly affect EEJ during CIR events on occasions
- The geoeffectiveness of CIR events are evaluated in terms of these prompt penetration periodicities in the equatorial ionosphere
- The CIRs are found to be geoeffective when the average solar wind flow is radial to within 6degrees

Correspondence to:
D. Rout,
diptir@prl.res.in

Citation:
Rout, D., D. Chakrabarty, P. Janardhan, R. Sekar, V. Maniya, and K. Pandey (2017), Solar wind flow angle and geoeffectiveness of corotating interaction regions: First results, *Geophys. Res. Lett.*, *44*, 4532–4539, doi:10.1002/2017GL073038.

Received 10 FEB 2017
Accepted 1 MAY 2017
Accepted article online 4 MAY 2017
Published online 27 MAY 2017

Solar wind flow angle and geoeffectiveness of corotating interaction regions: First results

Diptiranjan Rout[1], D. Chakrabarty[1], P. Janardhan[1], R. Sekar[1], Vrunda Maniya[1], and Kuldeep Pandey[1]

[1]Physical Research Laboratory, Ahmedabad, India

Abstract A total of 43 Corotating Interaction Region (CIR)-induced geomagnetic storms during the unusually deep solar minimum of solar cycle 23 (2006–2010) were identified using a superposed epoch analysis technique. Of these 43 events, detailed cross-spectrum analyses, between the variations in the *Z* component of the interplanetary magnetic field (IMF B_z) and the equatorial electrojet (EEJ) strength, were performed for 22 events when the daytime EEJ strengths from Jicamarca were available. The analyses revealed that the ~30 and ~60 min periodic components in IMF B_z were causally related to the EEJ strength subject to the average solar wind flow being radial to within 6° at L1 during the interval for which EEJ strengths were considered. This investigation elicits the important role of average solar wind azimuthal flow angle in determining the geoeffectiveness of CIR events.

Plain Language Summary Corotating Interaction Regions (CIRs) can disturb the near-Earth geospace significantly as the charged particles are accelerated in the shocked region in the interplanetary medium due to the passage of CIR and these energetic particles can reach Earth's orbit. Satellites are vulnerable to these high-energy particles during CIRs. In a technologically developed/developing society, the health of its satellites in the near-Earth space is crucial. Therefore, determining the geoeffectiveness of CIR is important.

1. Introduction

It is well known that the fast solar wind (600–800 km s^{-1}) originates in high-latitude coronal holes, while the slow speed solar wind (300–400 km s^{-1}) is confined to the low-latitude equatorial belt [*Ananthakrishnan et al.*, 1995]. The fast solar wind interacts with the slow stream solar wind near the ecliptic plane in the interplanetary medium creating an interaction region generally known as a "Corotating Interaction Region" or CIR [*Tsurutani et al.*, 2006; *Denton et al.*, 2006]. In a CIR, the stream interface is conventionally identified by increases in solar wind velocity and proton temperature, a sharp drop in proton density as well as shear in solar wind flow that can make the flow angle nonradial [*Forsyth and Marsch*, 1999; *Tsurutani et al.*, 1995]. The interaction regions are long-lived, have intense magnetic field, and corotate with the Sun and are bounded by forward and reverse shock regions. It has been suggested by *Pizzo* [1989] that for a corotating solar wind structure, the interface acts like a wall or an obstacle thereby deflecting the impinging solar wind and making it nonradial. However, the deviation from the radial nature of the solar wind is in general not very significant, with azimuthal velocities being usually between 30 and 50 km s^{-1} and nonradial flow angles rarely exceeding 10°. Some extreme cases of long-lasting nonradial solar wind outflows have, however, been reported when azimuthal flow velocities exceeded 100 km s^{-1} [*Janardhan et al.*, 2005, 2008]. Such events are small in number and may not be a conventional CIR in terms of their generation mechanism. In present work, no attempt is made to address this aspect, and only characteristic changes in solar wind parameters, as discussed above, are only used to identify the CIR or CIR-like events.

It is also known that the Alfvénic waves associated with the high-speed streams [*Burns et al.*, 2012] cause fast fluctuations in the interplanetary magnetic field (IMF). In a CIR, such Alfvénic fluctuations are expected to affect the equatorial ionosphere nearly instantaneously, if the rate of change of the IMF B_z fluctuations (or in other words, fluctuations in the dawn-dusk component of interplanetary electric field or IEFy) is faster than the shielding time constant [e.g., *Senior and Blanc*, 1984] at the inner edge of the ring current region. The electric

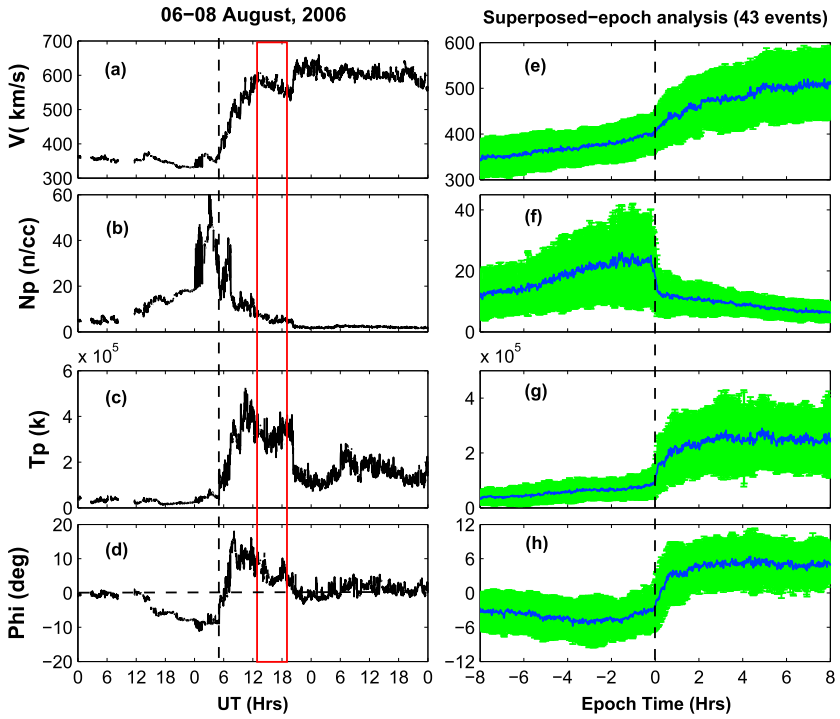

Figure 1. Variations in (a) solar wind flow velocity (V in km/s), (b) proton density (N_p in cm^{-3}), (c) proton temperature (T_p in K), and (d) flow angle (Φ in degrees) during 6–8 August 2006. The stream interface is marked by the vertical dotted line at ~0510 UT. Superposed epoch analyses for (e) V, (f) T_p, (g) N_p, and (h) Φ for all the 43 events are shown. The dashed line represents zero epoch time. The green envelop represents the standard deviations from the mean values.

field perturbations that arise from the fast fluctuations in IEFy are generically known as prompt penetration (PP) electric field [e.g., *Kelley et al.*, 2003]. As the solar wind speed remains relatively steady compared to the fast fluctuations in IMF B_z, the fluctuations in IEFy or convection electric filed can be attributed to the fluctuations in IMF B_z.

A comprehensive knowledge about the PP electric field periodicities during CIR events can be used to gauge their geoeffectiveness. Though the impacts of the CIR events on ionosphere and thermosphere, with periodicity of the order of solar rotational period (27 days) and its subharmonics (e.g., 27 days, 13.5 days, and 9 days) have been reported [e.g., *Lei et al.*, 2008; *Pedatella et al.*, 2010], signatures of the same periodic components have not been found in EEJ (driven primarily by the zonal electric field) that flows in the dip equatorial E region [*Tulasi Ram et al.*, 2012]. In fact, as far as the effects of the CIR-related fast fluctuating (period $\leq$ 2.0 h) components in IMF B_z on the equatorial ionosphere are concerned, which are generically associated with PP events, there has been a real dearth of comprehensive investigation. The geoeffectiveness of CIR events in terms of their impact on the equatorial ionosphere is also poorly understood. Given this context, the present investigation is important on two counts as it shows, for the first time, the key role played by the solar wind flow angle in determining the geoeffectiveness of the CIR events and also brings out the periodic components ($\leq$2.0 h) in CIR that affect EEJ.

2. Data Analysis and Result

A total of 43 minor geomagnetic storm events during 2006–2010, the deep solar minimum of solar cycle 23, were selected for the present investigation in which the stream interface was identified following the methodology discussed in *Forsyth and Marsch* [1999]. The solar wind parameters have been corrected for propagation lag till the bow shock nose. Figures 1a–1d show variations in solar wind flow velocity (V in km s^{-1}), proton density (N_p in cm^{-3}), proton temperature (T_p in K), and flow angle ($\Phi = \tan^{-1}\left(\frac{Vy}{Vx}\right)$ in degrees) for one such event during 6–8 August 2006. The stream interface is marked by the vertical dotted line at ~0510 UT. The characteristic increases in V and T_p, drop in N_p, and the change in Φ downstream of the stream interface region

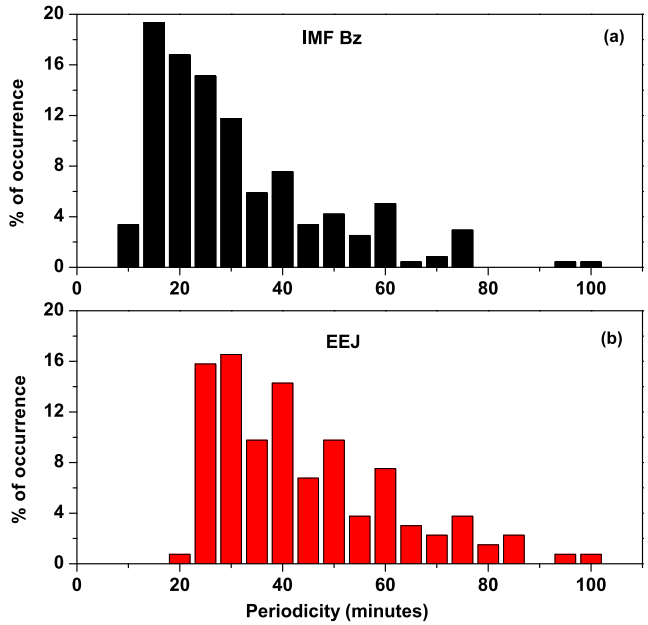

Figure 2. Histograms of (a) IMF B_z and (b) EEJ periodicities.

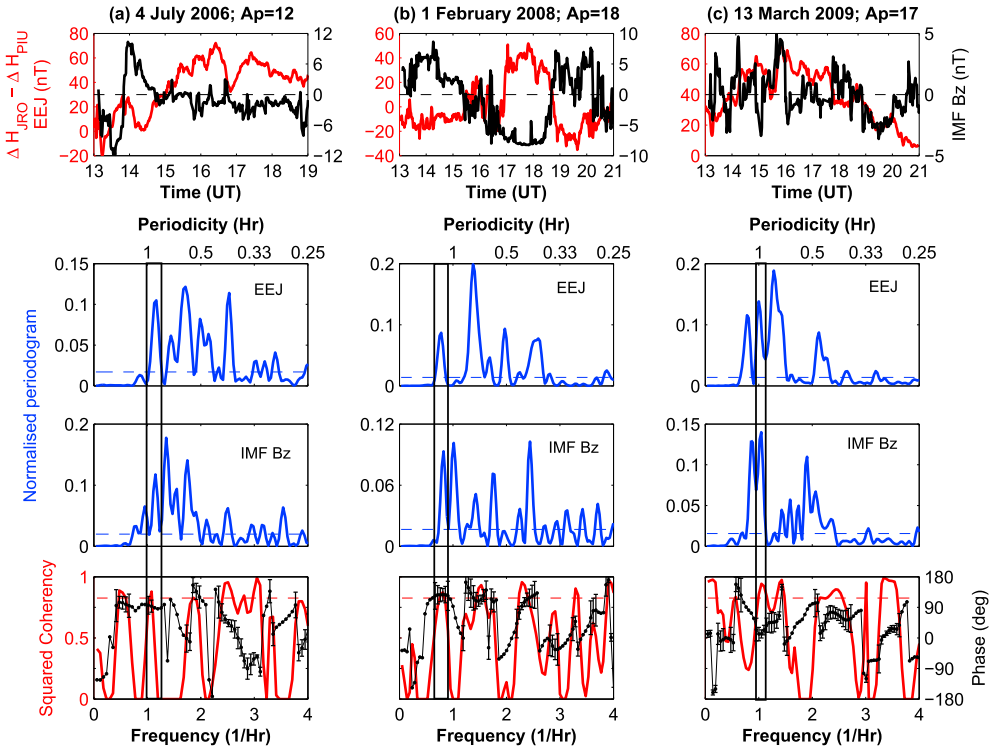

Figure 3. (a) The top panel shows the temporal variations of EEJ (red) and IMF B_z (black) during 1300–1900 UT on 4 July 2006; the middle two panels show the Lomb-Scargle normalized periodograms for EEJ and IMF B_z where the blue horizontal line shows the 95% confidence limit, and the bottom panel represents the squared coherency (red) with the phase spectra (black) for the two time series. The false alarm level is marked at 80% and is shown by a red dashed line. (b and c) Similar results as Figure 3a but for the other two events on 1 February 2008 and 13 March 2009 during 1300–2100 UT. The rectangular box is marked to show the common periodic components where the time series of EEJ and IMF B_z show significant coherency with stable phase relationship (essential to infer causal relationship).

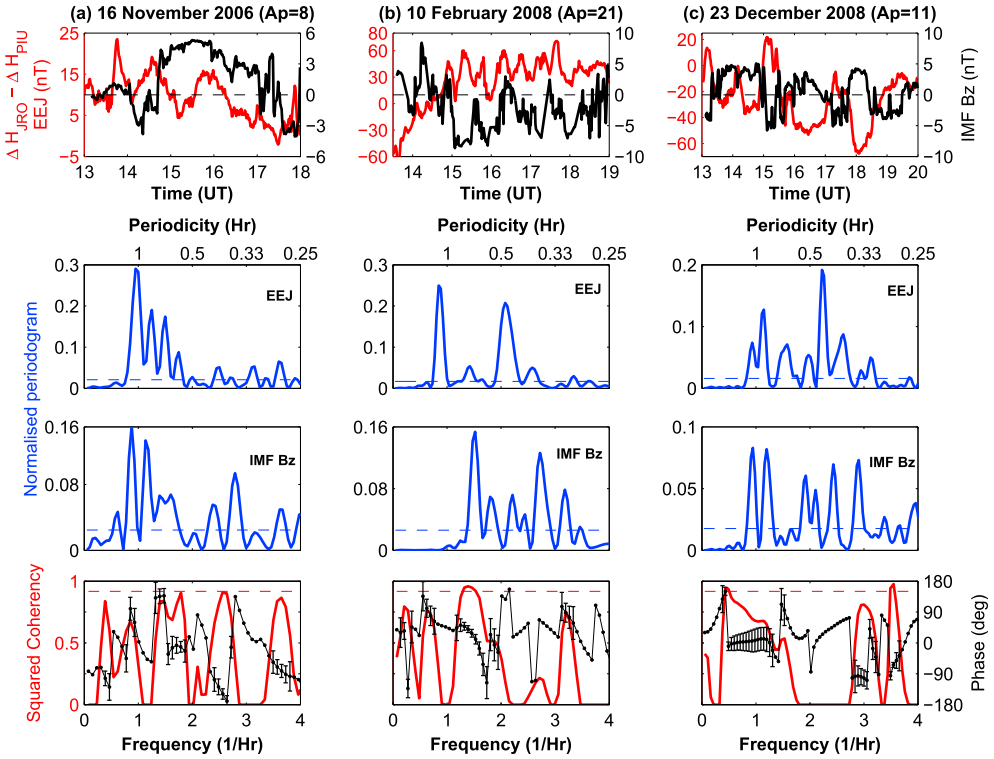

Figure 4. Same as Figure 3 but for (a) 16 November 2006 during 1300–1800 UT, (b) 10 February 2008 during 1330–1900 UT, and (c) 23 December 2008 during 1300–2000 UT, respectively. No causal relationship is noticed in these cases.

can be clearly seen. In order to extract the average trends of the solar wind parameters, a superposed epoch analysis was performed with the zero epoch corresponding to the time when the Earth is hit by the stream interface. Figures 1e–1h shows superposed epoch plots for V, T_p, N_p, and Φ for the 43 events and reveals the important characteristics of the stream interface typically associated with CIR events. The dashed line and the green envelope show, respectively, the zero epoch time and the standard deviation from the mean values.

3. Causal Connection Between IMF B_z and EEJ Strength During CIR Events

The EEJ strength over the Jicamarca sector, given by ΔH_{JIC}-ΔH_{PIU}, is based on the difference between the horizontal component of geomagnetic field over Jicamarca (JIC: 12°S, 76.8°W, 0.8° dip) and an off-equatorial station Piura (PIU: 5.2°S, 80.6°W, 6.8° dip). For Jicamarca, the local time (LT) = Universal time (UT) − 5 h. The EEJ strength over Jicamarca was shown to be same with the variations deduced by JULIA radar for the ionospheric E region electric field [*Alken and Maus*, 2010]. EEJ data with 1 min resolution during 1300–2100 UT (0800–1600 LT) were considered. As the EEJ data are available only during daytime, the investigation was restricted to 22 out of 43 events considered.

The fast (≤ 2.0 h) fluctuations (residuals) in EEJ and IMF B_z during these events were extracted (by detrending) using the Savitzky-Golay (SG) smoothing algorithm [*Savitzky and Golay*, 1964]. In order to know the dominant periodicities present in IMF B_z and EEJ, a detailed spectral analysis was carried out by using the standard Lomb-Scargle method [*Schulz and Stattegger*, 1997] which can handle unevenly sampled data. Only periodicities exceeding the 95% confidence limit were considered. Histograms with 5 min bin size based on the periodicities obtained from IMF B_z and EEJ residual time series data for 22 events are shown in Figures 2a and 2b, respectively. It is to be noted here that the lower cutoff periodicity in this case is chosen to be 10 min as the Brunt-Vaisala period at E region height is ~5 min. Further, it is known that Alfvénic waves in CIR with periods more than 8 min [e.g., *Korth et al.*, 2011] can efficiently affect ionosphere. As the EEJ data are available mostly for 6–8 h, periodicities ≤ 2.0 h can safely be addressed. It is clear from the histograms that the two most

Table 1. A Numbered (Column 1), Dated (Column 2) List of Events Showing Coherent Periodicities of Prompt Penetration Electric Field in Minutes (Column 3) Having Stable Phase Relationship and the Azimuthal Flow Angle | Φ | in Degrees (Column 4)[a]

Event	Date	Periodicities (min) of Prompt Penetration Electric Field	Average | Φ | (deg)
1	9 Apr 2006	27	5.1
2	15 Jun 2006	25	2.1
3	4 Jul 2006	60	1.0
4	7 Aug 2006	60	5.3
5	7 May 2007	46	3.8
6	20 Nov 2007	48	2.3
7	31 Jan 2008	37	1.3
8	1 Feb 2008	70	5.4
9	22 Jul 2008	30	5.7
10	23 Jul 2008	32	4.4
11	7 Nov 2008	60	3.1
12	13 Mar 2009	60	3.7
13	11 Nov 2010	60	1.7
15	20 Feb 2006	-	9.6
17	18 May 2006	-	6.4
14	17 Dec 2007	-	6.3
16	5 Jan 2008	-	6.6
18	10 Feb 2008	-	6.3
19	23 Dec 2008	-	6.2
21	16 Nov 2006	-	5.3
20	6 Aug 2009	53	6.8
22	26 Jun 2010	-	2.4

[a]Out of 22 events, 13 show a causal relationship between IMF B_z and EEJ, and these are shown in black. Events with common periodicities that do not show any causal relationship are shown in red, and events for which the flow angle criterion was ineffective are shown in blue. The absence of causal relationship is marked by a dash.

dominant periodic components in EEJ are 25 and 30 min, whereas in case of IMF B_z, the dominant periodic components are 15 and 20 min during the CIR events. In fact, some other common significant periodicities (30, 40, 50, and 60 min) are also present in both the parameters.

In order to establish the causal relationship between IMF B_z and EEJ, cross-spectrum analyses with coherency and phase spectra calculations were carried out [*Schulz and Stattegger*, 1997]. In Figure 3a, the top panel shows the temporal variations of EEJ (red) and IMF B_z (black) during 1300–1900 UT on 4 July 2006 (Ap = 12). The middle two panels show the normalized periodograms for EEJ and IMF B_z where the blue horizontal line is marked at 95% confidence limit, and the bottom panel represents the squared coherency (red) with the phase spectra (black) for the two time series. The false alarm level is marked at 80% (red dashed line). Figures 3b and 3c show the similar results for the other two events on 1 February 2008 (Ap = 18) and 13 March 2009 (Ap = 17) during 1300–2100 UT. The rectangular box is marked to show the common periodic components where the time series of EEJ and IMF B_z show significant coherency with stable phase relationship (essential to infer causal relationship). The periodicity of 60 min is found to be causally connected on 4 July 2006. Similarly, the periodicities of 70 min and 60 min in EEJ are found to be causally connected with IMF B_z on 1 February 2008 and 13 March 2009, respectively. Though there are multiple common periodicities present in both the parameters, only a few periodic components in EEJ are found to be responding to the corresponding fluctuations in IMF B_z. It is to be noted that on many occasions (Figure 3), periodicities adjacent to the causally connected ones do not show either high coherency and/or stable phase relationship. This probably indicates

sharp frequency response as far as the magnetosphere-ionosphere (M-I) coupling is concerned. Figure 4 is the same as Figure 3, but for (a) 16 November 2006 ($Ap = 8$) during 1300–1800 UT, (b) 10 February 2008 ($Ap = 21$) during 1330–1900 UT, and (c) 23 December 2008 ($Ap = 11$) during 1300–2000 UT, respectively. In all these cases, both EEJ and IMF B_z show fast fluctuations and they have common periodicities as well. As an example, one can take the case shown in Figure 4a wherein the 60 min periodicity is present in both IMF B_z and EEJ on 16 November 2006, but they are not causally related as neither the coherency is high nor the phase relationship is stable.

4. Causal Connection and Solar Wind Azimuthal Flow Angle

In Figures 1a–1d, the red rectangular box is marked for a typical event where the EEJ data have been analyzed (1300–1900 UT on 7 August 2006). For all the events considered, the modulus of the average value of the solar wind azimuthal flow angle ($|\ \Phi\ |$ in degrees) during this interval was calculated. Table 1 provides the date of events, periodicities (in min) of prompt penetration electric field (with stable phase relationship) and $|\ \Phi\ |$. The absence of any causal relationship is marked by a dash in the table. It can be noted from Table 1 that 13 out of 22 events have shown causal relationship between IMF B_z and EEJ at different periodicities wherein $|\ \Phi\ | < 6°$. These events are marked in black. The six events that do not show any causal relationship (though they have common periodicities) are marked in red in Table 1. For these events, $|\ \Phi\ | > 6°$. Among all these periodicities, ~60 and ~30 min periodic components have occurred five and four times, respectively. In fact, in most of the cases these two periodic components in IMF B_z (IEFy) are found to affect EEJ over the Jicamarca sector. Therefore, out of all 22 events, this criterion of solar wind flow angle determining geoeffectiveness was found to be valid for 19 events (86.4% of the total cases considered). These events are marked in blue in Table 1.

5. Discussion

The histogram in Figure 2b emphasizes the fast fluctuating components present in IMF B_z during the CIR events. The periodicities in IMF including the most dominant periodicities, in the range of 15–25 min, are associated with the Alfvénic fluctuations in IMF [e.g., *Tsurutani et al.*, 2006; *Korth et al.*, 2011] in CIR. It may be noted that the percentage occurrence of 20 min periodicity is very small (in contrast to quite time feature as reported by *Reddy and Devasia* [1976], for example) in EEJ although the same periodicity is quite dominant in IMF B_z. This may be associated with the EEJ during disturbed condition. It is known that although IMF B_z (or IEFy) comprises a wide range of periodicities, only a few periodic fluctuations affect low/equatorial ionosphere. The periodicity in IMF B_z that affects low latitude depends on the shielding process at the inner edge of the ring current. The typical shielding time constant is ~30 min [e.g., *Senior and Blanc*, 1984]. However, earlier observations reveal that shielding can remain broken for longer duration of time [*Huang et al.*, 2005; *Chakrabarty et al.*, 2015]. Therefore, although it is clear that the frequency response around the ring current region decides the prompt penetration frequency, the nature [e.g., *Ohtani and Uozumi*, 2014] of the processes that controls this response is not comprehensively understood. Nevertheless, the present study (Table 1) shows that on some occasions, DP2 (30 and 60 min periodicities) type [*Nishida*, 1968; *Sastri et al.*, 2000; *Chakrabarty et al.*, 2008, 2015] periodic fluctuations can reach up to dip equatorial ionosphere in daytime during the passage of CIRs.

Table 1 suggests that the presence of PP electric field during CIR depends on the azimuthal solar wind flow angle (Φ) with the events which do not show causal relationship between EEJ and IMF B_z, having $|\ \Phi\ |$ more than 6°. This is strikingly valid barring three events studied in this work. In other words, when the solar wind flow becomes nonradial (in the ecliptic plane) beyond a critical angle (6°), the dayside merging of IMF B_z with the geomagnetic field becomes less efficient. The importance of this critical angle can be evaluated geometrically by invoking the typical size of the dayside magnetopause and by using the flow angle at the L1 point from where the CIR observations are made. Considering the azimuthal flow angle, $|\ \Phi\ | = 6°$, and the distance of the L1 point to be ~232 R_E (1 R_E = 6371 km), the dawn/dusk flank of magnetopause turns out to be ~25 R_E away. This extends beyond the magnetopause flank that can be typically taken to be ~20 R_E [e.g., *Walsh et al.*, 2012] away from the center of the Earth. This essentially means that the CIR will miss the magnetopause if Φ exceeds 6° assuming the CIRs undergo no further interaction between the L1 point and the magnetopause. Under this scenario, the probability of merging of IMF B_z with the terrestrial magnetic field decreases significantly. As a consequence, the geoeffectiveness of the CIR events decreases drastically as the flow angle exceeds 6° which is the highlight of the present investigation. It is, therefore, expected that prompt penetration occurs only on those cases when the solar wind flow angle is within 6°.

At this juncture, it is important to note that once the solar wind hits the magnetopause at angles less than 6°, two mechanisms can be invoked to explain the dayside merging process. The dayside merging process is mediated through the merging electric field [e.g., *Kan and Lee*, 1979; *Siscoe and Crooker*, 1974] which is defined as $E_r = V_{SW}B_T Sin^2\theta/2$, where θ is the clock angle, V_{SW} is the solar wind velocity, and B_T is the total magnetic field. The merging electric field is generally believed to operate on a macroscopic scale. This is supported by the works of *Fejer et al.* [2007] and *Wei et al.* [2008] that suggest the critical role of merging electric field in M-I coupling. On the other hand, it was shown [*Borovsky*, 2008; *Borovsky et al.*, 2008; *Borovsky and Birn*, 2014] that the merging electric field is controlled by the local plasma parameters in the magnetosheath and magnetosphere, and these plasma parameters are controlled by the solar wind conditions. Hence, it was argued by them that the parameters in the solar wind decide the merging electric field. Recently, it has been experimentally observed [*Zhang*, 2016] that the reconnection takes place in an asymmetric medium as the plasma parameters are not same on the bow shock and magnetopause side of the magnetosheath region. Therefore, depending on the local plasma processes, the merging can be different on some occasions even if the flow angle is well within 6°. This probably explains the anomalous cases (see Table 1) reported in this work wherein the flow angle is less than 6° but the associated CIRs do not affect the equatorial ionosphere. This proposition is consistent with the solar wind-magnetosphere coupling mechanism suggested by *Borovsky* [2008].

The important role of the flow angle gets further support from the results of *Oliveira and Raeder* [2015] who showed that IP shocks with similar upstream conditions (such as magnetic field, speed, density, and Mach number) can have different levels of geoeffectiveness, depending on their shock normal orientation (which can change if the flow angle changes). Therefore, it is apparent that the solar wind flow angle at the L1 point plays a key role in determining geoeffectiveness of CIR events.

6. Summary

The present investigation suggests that 30 and 60 min periodicities in IMF B_z are efficient in penetrating into the equatorial ionosphere during CIR events as long as the solar wind azimuthal flow angle is less than ~6° at the L1 point. This is attributed to the reduction in the merging electric field in the dayside magnetosphere that occurs when the solar wind flow angle increases beyond a threshold. Therefore, this work provides a quick and easy method to forecast the geoeffectiveness of CIR events based on the observations from the L1 point.

Acknowledgments
The magnetic data over Jicamarca used in this work were taken from Madrigal Database at Jicamarca Radio Observatory (http://jro1.igp.gob.pe/madrigal/). The Jicamarca Radio Observatory is a facility of the Instituto Geofisico del Peru operated with support from the NSFAGS-1433968 through Cornell University. Special thanks are due to Marco Milla for allowing us to use the magnetometer data. The geomagnetic indices and solar wind data were obtained from NASA GSFC CDAWeb (http://cdaweb.gsfc.nasa.gov/istp_public/). We thank Madhusudan Ingale for helping us in making schematic diagram. This work is supported by the Department of Space, Government of India.

References

Alken, P., and S. Maus (2010), Relationship between the ionospheric eastward electric field and the equatorial electrojet, *Geophys. Res. Lett.*, *37*, L04104, doi:10.1029/2009GL041989.

Ananthakrishnan, S., V. Balasubramanian, and P. Janardhan (1995), Latitudinal variation of solar wind velocity, *Space Sci. Rev.*, *72*(1), 229–232, doi:10.1007/BF00768784.

Borovsky, J. E. (2008), The rudiments of a theory of solar wind/magnetosphere coupling derived from first principles, *J. Geophys. Res.*, *113*, A08228, doi:10.1029/2007JA012646.

Borovsky, J. E., and J. Birn (2014), The solar wind electric field does not control the dayside reconnection rate, *J. Geophys. Res. Space Physics*, *119*, 751–760, doi:10.1002/2013JA019193.

Borovsky, J. E., M. Hesse, J. Birn, and M. M. Kuznetsova (2008), What determines the reconnection rate at the dayside magnetosphere?, *J. Geophys. Res.*, *113*, A07210, doi:10.1029/2007JA012645.

Burns, A., S. Solomon, L. Qian, W. Wang, B. Emery, M. Wiltberger, and D. Weimer (2012), The effects of corotating interaction region/high speed stream storms on the thermosphere and ionosphere during the last solar minimum, *J. Atmos. Sol. Terr. Phys.*, *83*, 79–87, doi:10.1016/j.jastp.2012.02.006.

Chakrabarty, D., R. Sekar, J. H. Sastri, and S. Ravindran (2008), Distinctive effects of interplanetary electric field and substorm on nighttime equatorial f layer: A case study, *Geophys. Res. Lett.*, *35*, L19108, doi:10.1029/2008GL035415.

Chakrabarty, D., D. Rout, R. Sekar, R. Narayanan, G. D. Reeves, T. K. Pant, B. Veenadhari, and K. Shiokawa (2015), Three different types of electric field disturbances affecting equatorial ionosphere during a long-duration prompt penetration event, *J. Geophys. Res. Space Physics*, *120*, 4993–5008, doi:10.1002/2014JA020759.

Denton, M. H., J. E. Borovsky, R. M. Skoug, M. F. Thomsen, B. Lavraud, M. G. Henderson, R. L. McPherron, J. C. Zhang, and M. W. Liemohn (2006), Geomagnetic storms driven by ICME- and CIR-dominated solar wind, *J. Geophys. Res.*, *111*, A07S07, doi:10.1029/2005JA011436.

Fejer, B. G., J. W. Jensen, T. Kikuchi, M. A. Abdu, and J. L. Chau (2007), Equatorial ionospheric electric fields during the November 2004 magnetic storm, *J. Geophys. Res.*, *112*, A10304, doi:10.1029/2007JA012376.

Forsyth, R., and E. Marsch (1999), Solar origin and interplanetary evolution of stream interfaces, *Space Sci. Rev.*, *89*(1), 7–20, doi:10.1023/A:1005235626013.

Huang, C.-S., J. C. Foster, and M. C. Kelley (2005), Long-duration penetration of the interplanetary electric field to the low-latitude ionosphere during the main phase of magnetic storms, *J. Geophys. Res.*, *110*, A11309, doi:10.1029/2005JA011202.

Janardhan, P., K. Fujiki, M. Kojima, M. Tokumaru, and K. Hakamada (2005), Resolving the enigmatic solar wind disappearance event of 11 May 1999, *J. Geophys. Res.*, *110*, A08101, doi:10.1029/2004JA010535.

Janardhan, P., D. Tripathi, and H. Mason (2008), The solar wind disappearance event of 11 May 1999: Source region evolution, *Astron. Astrophys.*, *488*(1), L1–L4.

Kan, J. R., and L. C. Lee (1979), Energy coupling function and solar wind-magnetosphere dynamo, *Geophys. Res. Lett.*, *6*(7), 577–580, doi:10.1029/GL006i007p00577.

Kelley, M. C., J. J. Makela, J. L. Chau, and M. J. Nicolls (2003), Penetration of the solar wind electric field into the magnetosphere/ionosphere system, *Geophys. Res. Lett.*, *30*(4), 1158, doi:10.1029/2002GL016321.

Korth, A., E. Echer, Q.-G. Zong, F. Guarnieri, M. Fraenz, and C. Mouikis (2011), The response of the polar cusp to a high-speed solar wind stream studied by a multispacecraft wavelet analysis, *J. Atmos. Sol. Terr. Phys.*, *73*(1), 52–60, doi:10.1016/j.jastp.2009.10.004.

Lei, J., J. P. Thayer, J. M. Forbes, E. K. Sutton, and R. S. Nerem (2008), Rotating solar coronal holes and periodic modulation of the upper atmosphere, *Geophys. Res. Lett.*, *35*, L10109, doi:10.1029/2008GL033875.

Nishida, A. (1968), Geomagnetic Dp 2 fluctuations and associated magnetospheric phenomena, *J. Geophys. Res.*, *73*(5), 1795–1803, doi:10.1029/JA073i005p01795.

Ohtani, S., and T. Uozumi (2014), Nightside magnetospheric current circuit: Time constants of the solar wind-magnetosphere coupling, *J. Geophys. Res. Space Physics*, *119*, 3558–3572, doi:10.1002/2013JA019680.

Oliveira, D. M., and J. Raeder (2015), Impact angle control of interplanetary shock geoeffectiveness: A statistical study, *J. Geophys. Res. Space Physics*, *120*, 4313–4323, doi:10.1002/2015JA021147.

Pedatella, N. M., J. Lei, J. P. Thayer, and J. M. Forbes (2010), Ionosphere response to recurrent geomagnetic activity: Local time dependency, *J. Geophys. Res.*, *115*, A02301, doi:10.1029/2009JA014712.

Pizzo, V. J. (1989), The evolution of corotating stream fronts near the ecliptic plane in the inner solar system: 1. Two dimensional fronts, *J. Geophys. Res.*, *94*(A7), 8673–8684, doi:10.1029/JA094iA07p08673.

Reddy, C., and C. Devasia (1976), Short period fluctuations of the equatorial electrojet, *Nature*, *261*(5559), 396–397.

Sastri, J., H. Luhr, H. Tachihara, T.-I. Kitamura, and J. V. S. V. Rao (2000), Letter to the editor electric field fluctuations (25–35 min) in the midnight dip equatorial ionosphere, *Ann. Geophys.*, *18*(2), 252–256, doi:10.1007/s00585-000-0252-2.

Savitzky, A., and M. J. Golay (1964), Smoothing and differentiation of data by simplified least squares procedures, *Anal. Chem.*, *36*(8), 1627–1639.

Schulz, M., and K. Stattegger (1997), Spectrum: Spectral analysis of unevenly spaced paleoclimatic time series, *Comput. Geosci.*, *23*(9), 929–945.

Senior, C., and M. Blanc (1984), On the control of magnetospheric convection by the spatial distribution of ionospheric conductivities, *J. Geophys. Res.*, *89*(A1), 261–284, doi:10.1029/JA089iA01p00261.

Siscoe, G., and N. Crooker (1974), A theoretical relation between Dst and the solar wind merging electric field, *Geophys. Res. Lett.*, *1*(1), 17–19, doi:10.1029/GL001i001p00017.

Tsurutani, B. T., W. D. Gonzalez, A. L. C. Gonzalez, F. Tang, J. K. Arballo, and M. Okada (1995), Interplanetary origin of geomagnetic activity in the declining phase of the solar cycle, *J. Geophys. Res.*, *100*(A11), 21,717–21,733, doi:10.1029/95JA01476.

Tsurutani, B. T., et al. (2006), Corotating solar wind streams and recurrent geomagnetic activity: A review, *J. Geophys. Res.*, *111*, A07S01, doi:10.1029/2005JA011273.

Tulasi Ram, S., M. Yamamoto, B. Veenadhari, S. Kumar, and S. Gurubaran (2012), Corotating interaction regions (CIRS) at sub-harmonic solar rotational periods and their impact on ionosphere-thermosphere system during the extreme low solar activity year 2008, *Indian J. Radio Space Phys.*, *41*, 294–245.

Walsh, B. M., D. G. Sibeck, Y. Wang, and D. H. Fairfield (2012), Dawn-dusk asymmetries in the Earth's magnetosheath, *J. Geophys. Res.*, *117*, A12211, doi:10.1029/2012JA018240.

Wei, Y., M. Hong, W. Wan, A. Du, J. Lei, B. Zhao, W. Wang, Z. Ren, and X. Yue (2008), Unusually long lasting multiple penetration of interplanetary electric field to equatorial ionosphere under oscillating IMF B_z, *Geophys. Res. Lett.*, *35*, L02102, doi:10.1029/2007GL032305.

Zhang, Y. (2016), Distinct characteristics of asymmetric magnetic reconnections: Observational results from the exhaust region at the dayside magnetopause, *Sci. Rep.*, *6*, 27592.